Supporting information

Proteome selectivity profiling of photoaffinity probes derived from imidazopyrazine-kinase inhibitors

Dimitris Korovesis,[1] Christel Mérillat,[1] Rita Derua,[2,3] and Steven H. L. Verhelst[*1]

[1] KU Leuven, Department of Cellular and Molecular Medicine, Laboratory of Chemical Biology, Herestraat 49 box 802, 3000 Leuven, Belgium

[2] KU Leuven, Department of Cellular and Molecular Medicine, Laboratory of Protein Phosphorylation and Proteomics, Herestraat 49 box 802, 3000 Leuven, Belgium

[3] KU Leuven, SyBioMa, Herestraat 49, 3000 Leuven, Belgium

*E-mail: steven.verhelst@kuleuven.be

Contents

Supplemental Figures

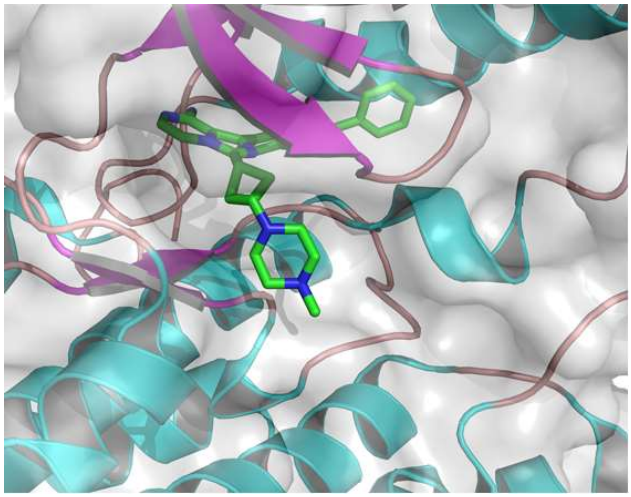

Figure S1. Co-crystal structure of IGF-1R with a linsitinib analogue (PDB: 3D94) shows that the *N*-substituent on the 4-membered ring points towards the solvent. The analog is depicted in sticks, and the protein in cartoon and semi-transparent surface representation. Picture rendered with PyMol.

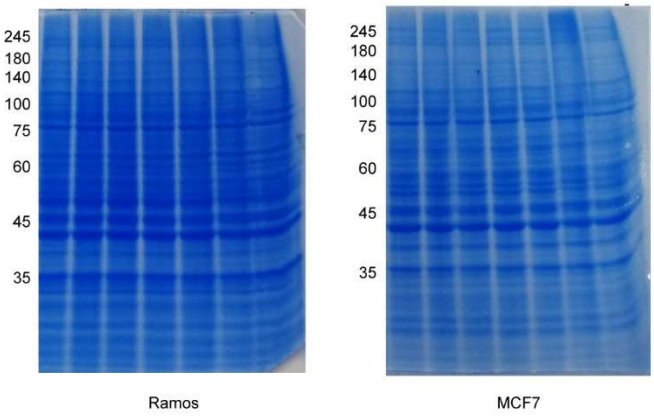

Figure S2. Coomassie stains of the gels displayed in main Figure 3A.

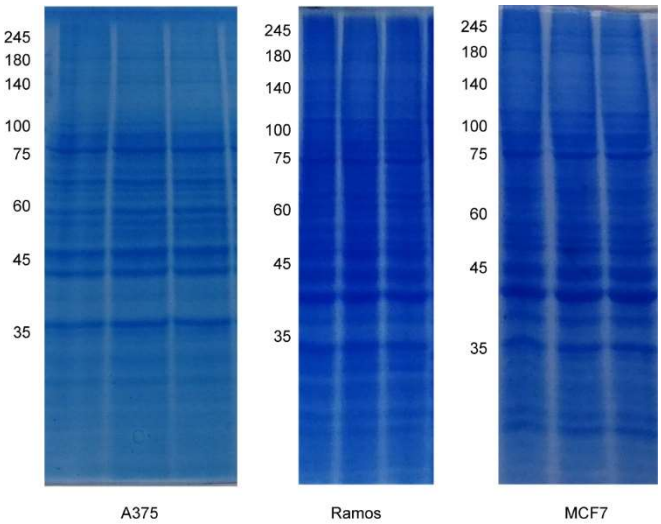

Figure S3. Coomassie stains of the gels displayed in main Figure 3B.

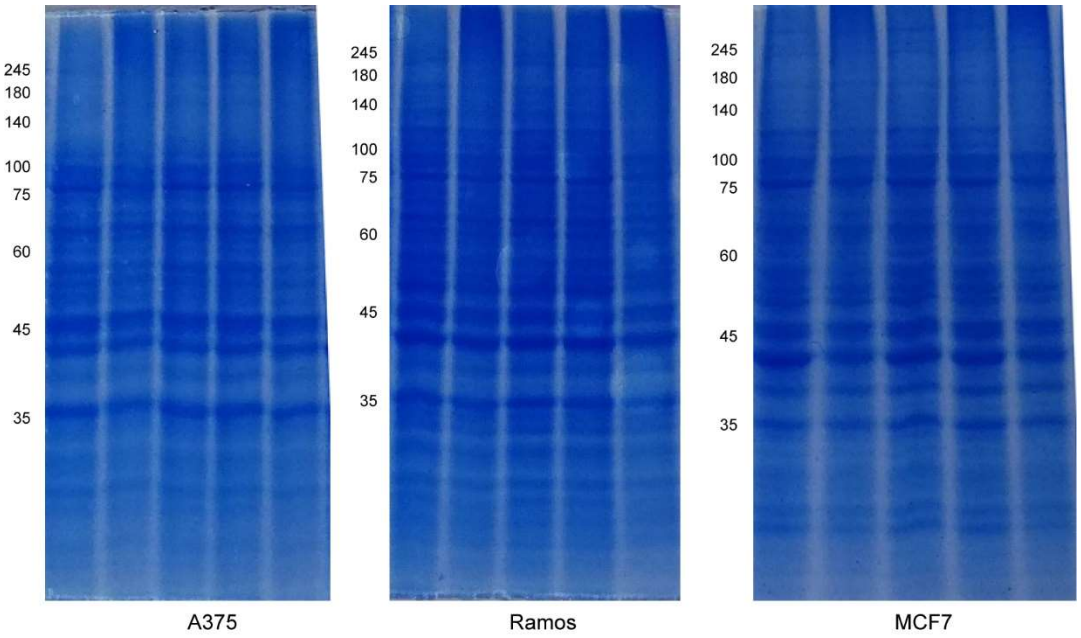

Figure S4. Coomassie stains of the gels displayed in main Figure 3C.

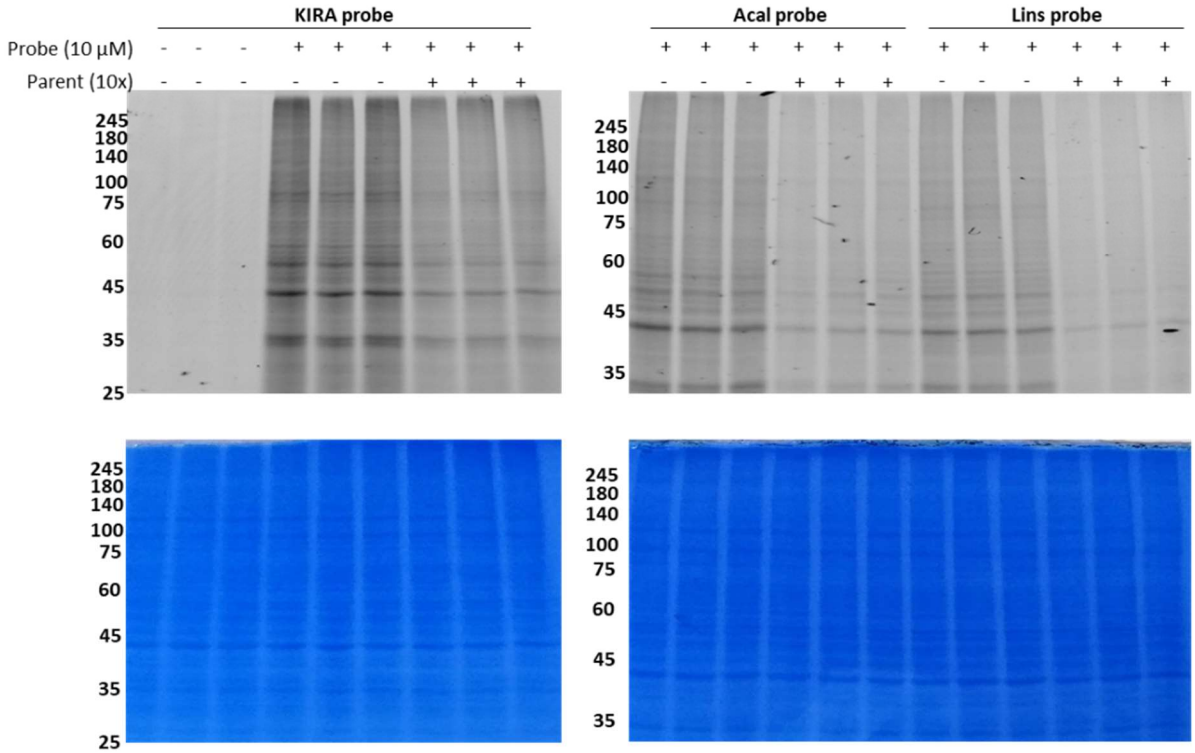

Figure S5. Quality control samples of labeling experiments that were subsequently processed for LC-MS/MS analysis.

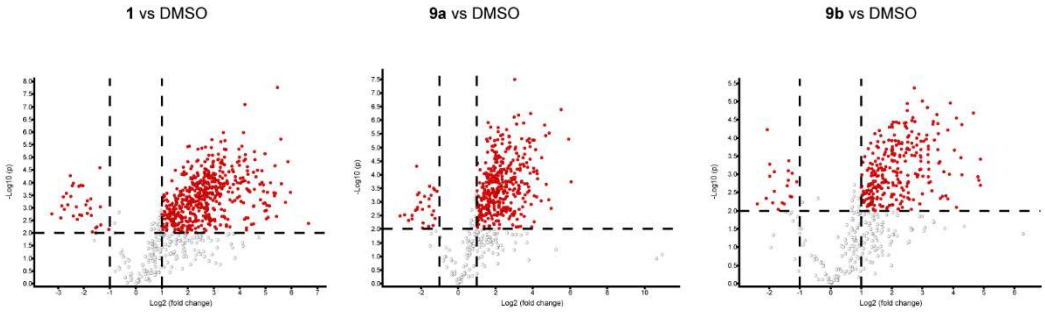

Figure S6. Volcano plots of significantly enriched proteins in the indicated probe sample versus dmso control. 2-fold enrichment and p-value of 0.01 were taken as cut-offs to determine hits in the upper right quadrant.

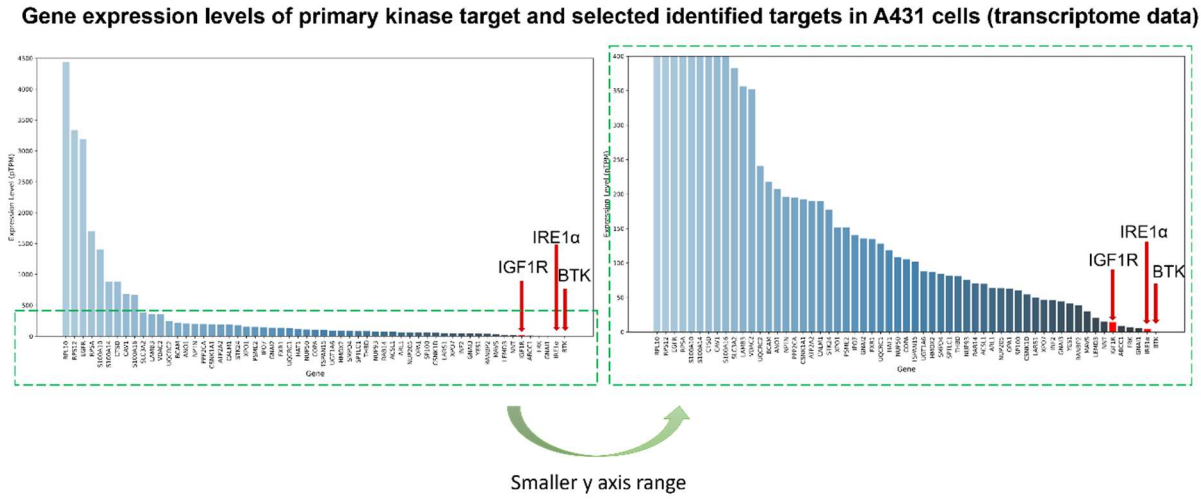

Figure S7. Expression in A431 cells of the primary targets and selected identified proteins in the proteomics identification experiments. Graphs depict transcriptome data from the human protein atlas[1]; y axis indicates number of mRNA transcripts per million. Note that the primary targets of the three probes (IGF1R, IRE1α and BTK) have very low expression, which clarifies why these were not identified by MS/MS.

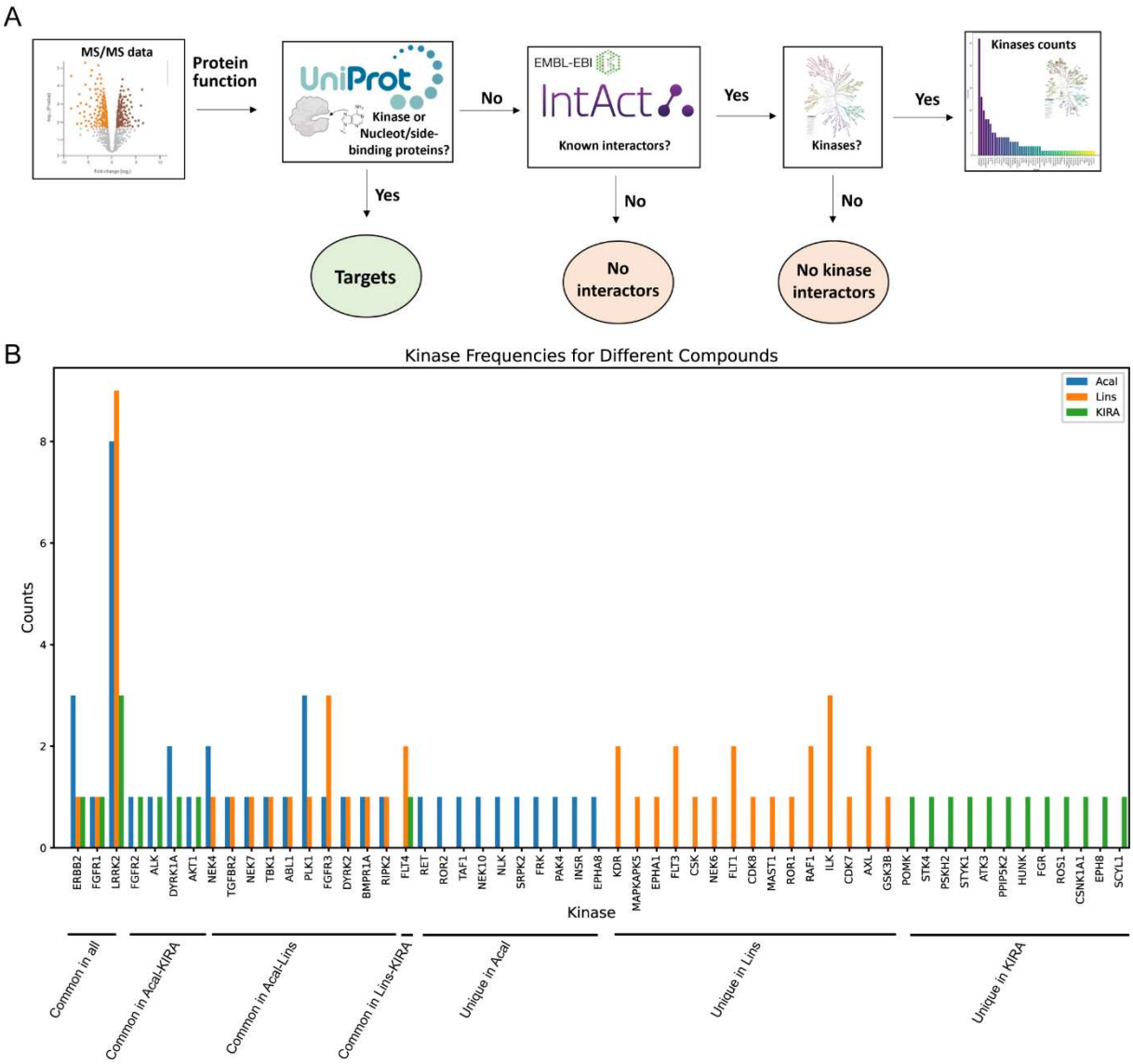

Figure S8. Analysis of target proteins. (A) Workflow of the automated protein target analysis. Protein hits from mass spectrometry analysis were classified based on function (i.e. match with relevant GO terms) as kinases, nucleotide/nucleoside binding proteins or others. Proteins in the "others" were submitted to the EMBL IntAct database to examine interactions with kinases. (B) Counts of interacting target proteins per kinase and per probe. For example, kinase LRRK2 is annotated in the IntAct database to interact with 8 of the identified targets of acalabrutinib probe **9a**, 9 of the identified targets of linsitinib probe **9b** and 2 of the identified targets of KIRA6 probe **1**. This analysis does not imply that all of these kinases are off-targets of the photoaffinity probes. Instead, we hypothesize that interactions between some of these kinases and some of the identified proteins may have led to their enrichment in the photoaffinity labeling workflow.

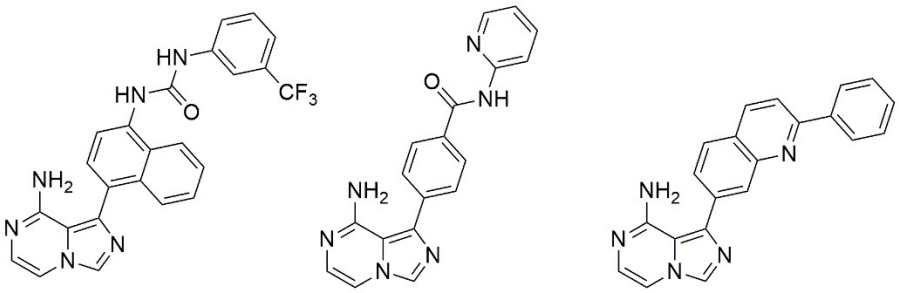

Figure S9. The scaffolds of KIRA6 (left), acalabrutinib (middle) and linsitinib (right) without the substituent at the 3-position, which were used for MD simulations and docking experiments to enable a focus on the effect of binding pocket-embedded substituents.

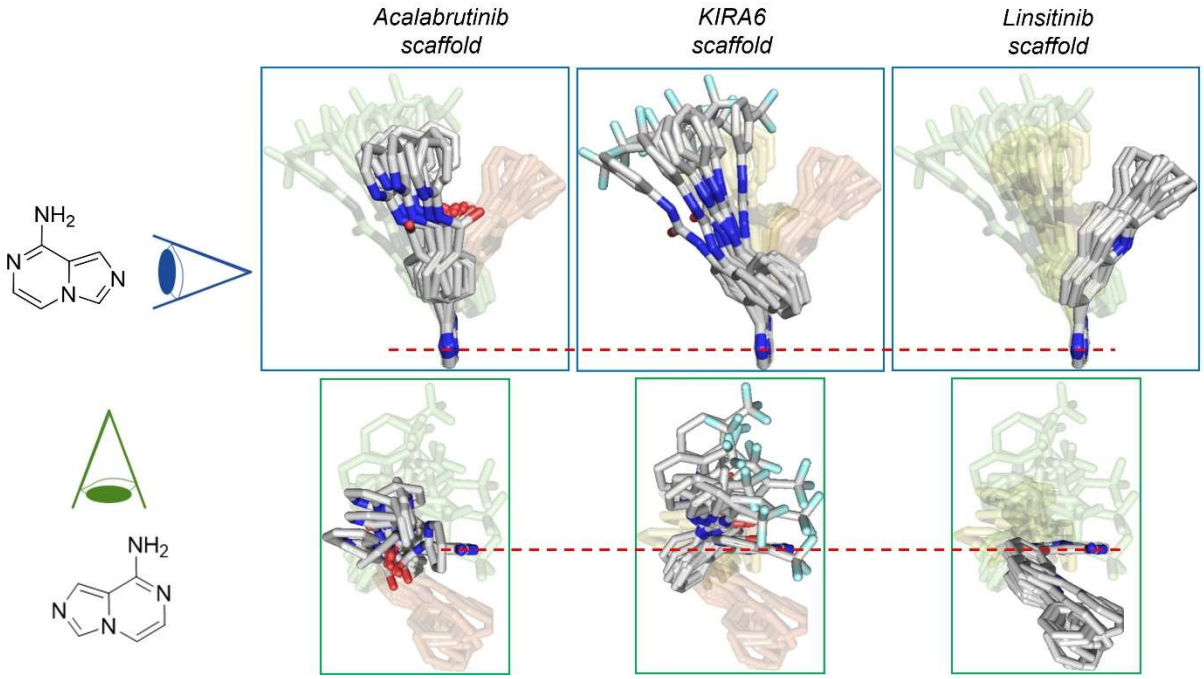

Figure S10. Visualization of the MD experiments on the acalabrutinib, KIRA6 and linsitinib scaffolds. For reasons of comparison, each picture contains the conformations of the other two scaffolds in yellow (acalabrutinib), pink (linsitinib) or green (KIRA6) shading, in a bounding box drawn based on all conformations. On the left, the direction of visualization is depicted. Note the higher conformational flexibility of KIRA6 and the rigidity of linsitinib, as well as the distinct orientation of the substituent on linsitinib.

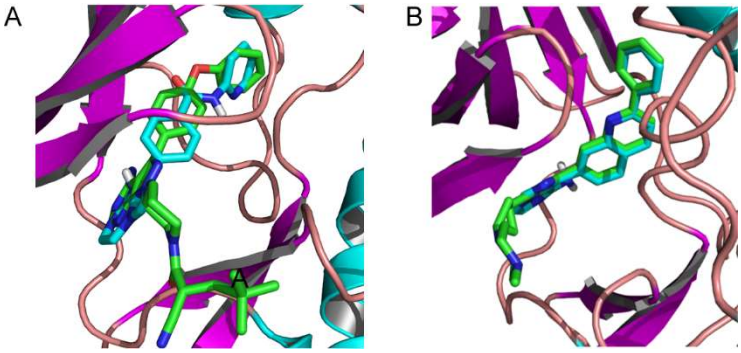

Figure S11. Docking of the imidazopyrazine scaffolds in the primary targets. Ligands are depicted in stick representations. The original ligand is colored in green, the docked scaffold in cyan. The protein is drawn in cartoon mode with magenta beta-sheets, cyan helices and pink random coils. Pictures rendered with PyMol. (A) acalabrutinib scaffold docked in BTK cocrystallized with a cyanoacrylamide inhibitor (PDB: 4YHF). (B) Linsitinib scaffold docked in IGF-1R (PDB 3D94).

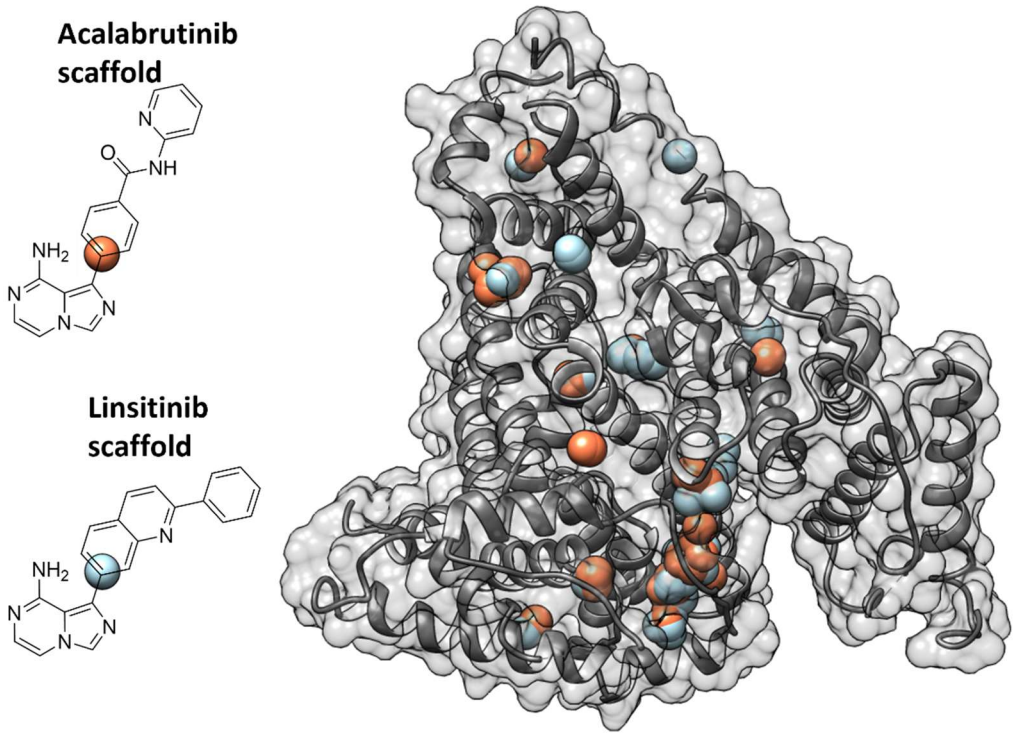

Figure S12. Docking against human serum albumin (PDB: 7WKZ) as negative control protein. A total of 90 poses were hierarchically clustered at the indicated carbon atom (orange or magenta spheres for the acalabrutinib and linsitinib scaffold, respectively) with a distance threshold of 8.0 Å were performed, where points within this distance were grouped into a cluster. Spheres within the crystal structure indicate the positions of these clusters. Note that the clusters are located at many different places on the HSA structure, indicating that the docking against this negative control target does not give any reasonable results.

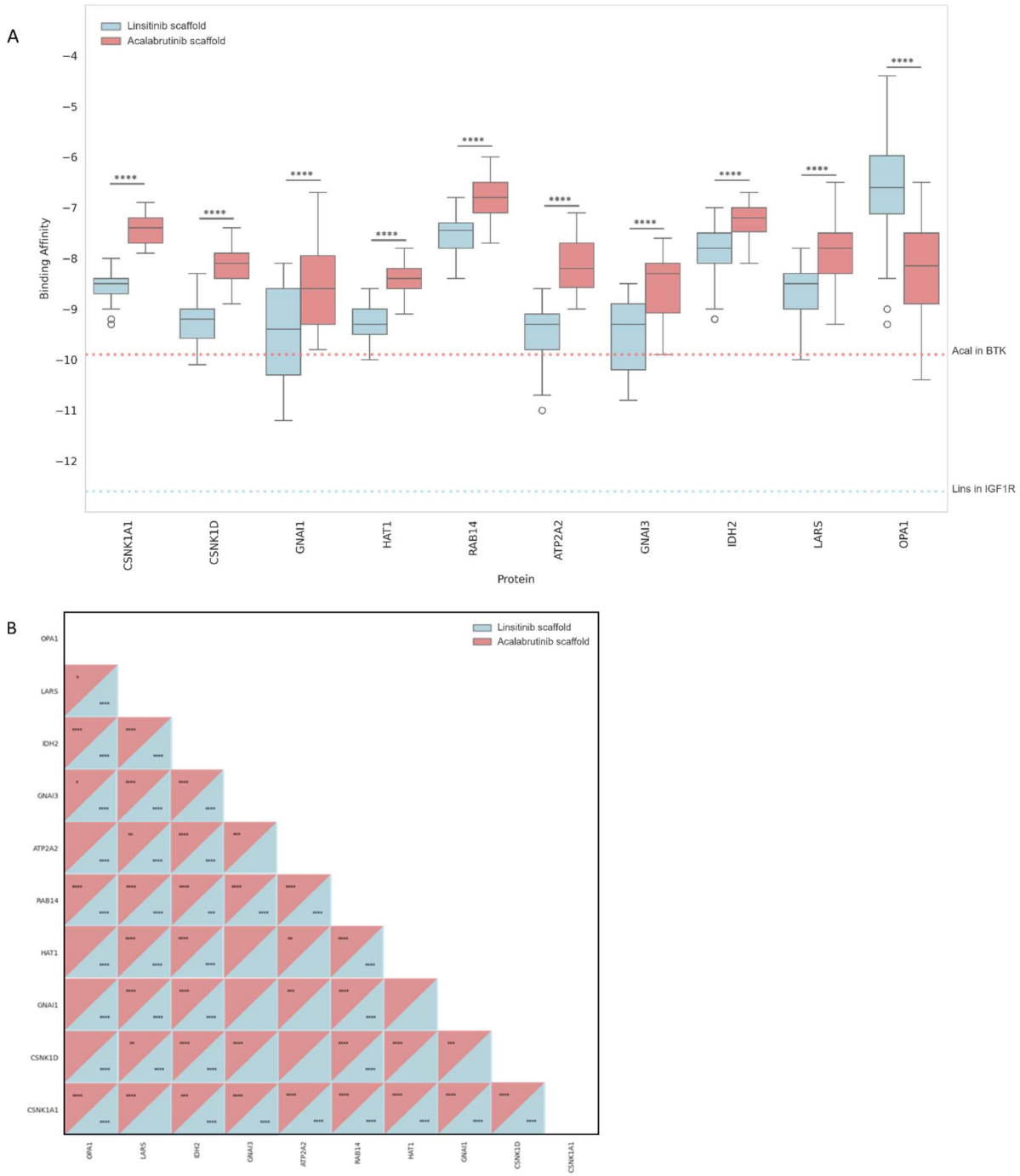

Figure S13. (A) Calculated binding affinity (kcal/mol) of the docked imidazopyrazine scaffolds (see Figure S9) in the crystal structure of the indicated protein (CSNK1A1: PDB 6GZD; CSNK1D: PDB 4HNF; GNAI1: PDB 5TDH; HAT1: PDB 2P0W; RAB14: PDB 4DRZ; ATP2A2: PDB 6JJU; GNAI3: PDB 4G5O; IDH2: PDB 6VFZ; LARS: PDB 6LPF; OPA1; PDB 6JTG Note that the average calculated binding affinity is consistently larger for the linsitinib scaffold, expect for the protein OPA1. Note that GNAI1 and HAT1 were found as targets of the acalabrutinib probe **9a**, but they also were found in the target identification of linsitinib probe

9b, albeit with only 1 unique peptide (for GNAI1) or a fold change in probe vs competition of 1.9 (for HAT1). Also note that the ATP2A2, GNAI3, IDH2, LARS and OPA1, which were found as targets of the linsitinib probe **9b**, were also found as targets of acalabrutinib probe **9a**, but with lower fold changes in probe vs competition (1.5, 1.9, 1.8, 1.6 and 1.6, respectively). Error bars represent the variability in calculated binding affinities across all docking poses, aggregated for each protein-molecule pair. The central line within each box indicates the median binding affinity, while the lightcoral and lightblue dotted lines show the median docking affinity of acalabrutinib against BTK and linsitinib against IGF1R, respectively, serving as positive controls. Statistical significance (Welch's t-test) between acalabrutinib and linsitinib binding affinities for each protein is indicated by stars (*), with four stars (***) denoting a p-value < 0.0001. (B) Pairwise significance matrix comparing binding affinities across protein targets for acalabrutinib and linsitinib scaffolds. Each cell represents the statistical significance between protein pairs, with acalabrutinib indicated as lightcoral (top left half of each cell) and linsitinib as lightblue (bottom right half). Stars indicate levels of significance based on p-values from pairwise (t-test) statistical tests.

Table S1 **Extended list of identified kinases** Red numbers indicate reasons for not being included in the final hitlist

Probe	Kinase included in hitlist?	Accession No	Gene name	Unique peptides	p value	fold change vs competitor	Found before?	Reference
1	Yes	B4DR80	STK24	9	$1.63 *10^{-3}$	3.82	Yes	10.1073/pnas.1906999116
1	Yes	P42685	FRK	2	$2.20*10^{-3}$	2.24	Yes	10.1073/pnas.1906999116
1	No	B4E0K5	MAPK14	1	$2.00*10^{-4}$	4.01	Yes	10.1073/pnas.1906999116
1	No	P12931	SRC	1	$4.27*10^{-3}$	2.21	No	
1	No	P29317	EPHA2	4	$4.03*10^{-4}$	1.69	No	
9a	Yes	B4DIJ9	N/A	5	$4.78*10^{-3}$	3.22	Yes	10.1021/acschembio.7b00617
9a	Yes	U3KPX3	CSNK1A1	8	$1.22*10^{-3}$	2.81	Yes	10.1021/acschembio.7b00617
9a	Yes	B2RA70	N/A (highly similar to YES)	3	$9,44*10^{-3}$	2.80	Yes	10.1021/acschembio.7b00617
9a	Yes	Q2TTR7	N/A (highly similar to EGFR)	42	$4.37*10^{-5}$	2.03	Yes	10.1021/acschembio.7b00617; 10.1124/jpet.117.242909
9a	No	A0A8I5KU53	MYLK	1	$3.84*10^{-5}$	3.74	Yes	10.1021/acschembio.7b00617
9a	No	D7RF68	N/A (highly similar to BRAF)	1	$3.38*10^{-3}$	1.71	Yes	10.1021/acschembio.7b00617
9a	No	H0Y630	STK24	1	$6.63*10^{-3}$	1.55	Yes	10.1021/acschembio.7b00617
9a	No	Q13308	PTK7	5	$5.08*10^{-3}$	1.47	No	
9a	No	P78527	PRKDC	37	$6.58*10^{-3}$	1.42	No	
9b	Yes	B2RA70	N/A (highly similar to YES)	3	$3.65*10^{-5}$	2.02	Yes	10.1074/jbc.M113.505032
9b	No	P29317	EPHA2 / ECK	5	$2.85*10^{-5}$	1.84	No	
9b	No	A0A0S2Z430	PCK2	13	$6.9*10^{-3}$	1.66	No	

Table S2: Identified proteins as interactors of kinase hits

Kinases in red were identified with less stringent criteria (see Table S2)

Probe	Kinase-interacting protein	Interacting kinase identified as hit
KIRA	DNCL1	STK24
	COPA	SRC
	HMOX2	SRC
Acal	GNAI1	EGFR
	DNCL1	CSNK1D, CSNK1A1, STK24
	RPSA	EGFR
	UQCRC1	YES
	CTSD	YES
	FXR1	YES
	RPL10	YES
	VDAC2	YES
	SLC3A2	EGFR
	PPP2CA	EGFR, STK24
	CALM1	EGFR
	SP100	CSNK1D
Lins	VDAC2	YES
	UQCRC1	YES
	UQCRC2	YES
	NPTN	YES
	XPO1	YES

Supplemental methods

General Chemistry

All starting materials and solvents were bought from commercial vendors and used without further purification. Reactions were analyzed by thin-layer chromatography (TLC) on precoated 0.20 mm thick ALUGRAM TLC sheets with a fluorescent indicator and by liquid chromatography-mass spectrometry (LC-MS) performed on a Prominence Ultra-fast Liquid Chromatography system equipped with a 2 × 150 mm C18 analytical column (Waters X-Bridge) coupled to an MS-2020 single-quadrupole mass analyzer (Shimadzu). Silica column chromatography was performed using 230–400 mesh silica (Kieselgel 60). High-pressure liquid chromatography (HPLC) purification was performed using a 10 × 150 mm C18 preparative column (X-Bridge). A linear gradient of 20–80% acetonitrile in water (with 0.1% TFA) was utilized. ^{1}H and ^{13}C NMR spectra were recorded on Bruker Ultra Shield Avance 300 MHz, 500 MHz or 600 MHz spectrometers using deuterated solvents. Chemical shifts (δ) on 1H spectra are relative to tetramethylsilane as internal standard and given in parts per million (ppm).

Compound 3a-b

In a flask containing (3-chloropyrazin-2-yl)methanamine (1.0 eq.) and carboxylic acid **10a-b** (1.05 eq.) in DCM (0.09 M), EDC hydrochloride (1.32 eq.), DIPEA (2.6 eq.) and DMAP (0.2 eq.) were added subsequently. After overnight stirring at rt, the reaction mixture was concentrated under vacuo. The residue was suspended in EtOAc and washed successively with sat. $NaHCO_3$, water and brine. The organic layer was dried over $MgSO_4$ and concentrated. The crude was purified by column chromatography (80% → 100% EtOAc in PE).

(*S*)-benzyl 2-(((3-chloropyrazin-2-yl)methyl)carbamoyl)pyrrolidine-1-carboxylate (3a)

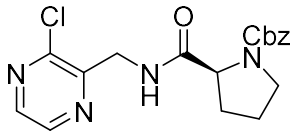

3a was obtained as a yellow oil (2.58 g, 6.9 mmol, 81%). R_f= 0.5 (100% EtOAc); ^{1}H NMR (300 MHz, $CDCl_3$) mixture of rotamers: δ 8.38 – 8.16 (m, 2H), 7.43 – 7.02 (m, 5H), 5.28 – 4.93 (m, 2H), 4.80 – 4.30 (m, 3H), 3.73 – 3.39 (m, 2H), 2.48 – 1.79 (m, 4H); ^{13}C NMR (75 MHz, $CDCl_3$) rotameric mixture, resonances for the minor rotamer are enclosed in parenthesis: δ 172.54, 154,93, 147.96, 142.37, 141.70 (141.45), 138.38, 128.31, 128.10, 127.95, 67.27, 61.15 (60.76), 47.56 (47.09), 41.85 (41.51), 31.20 (28.78), 24.59 (23.76). ESI-MS calcd for $C_{18}H_{20}ClN_4O_3^+$ 375.12 $[M+H]^+$, found 374.85.

Benzyl((1*s*,3*s*)-3-(((3-chloropyrazin-2-yl)methyl)carbamoyl)cyclobutyl)carbamate (3b)

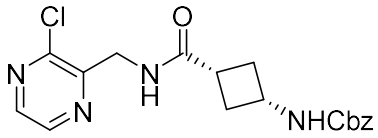

3b was obtained as a white solid (0.34 g, 0.9 mmol, 20%). R_f= 0.3 (80% EtOAc in PE); ^{1}H NMR (300 MHz, $CDCl_3$): δ 8.41 (d, *J* = 2.6 Hz, 1H), 8.28 (d, *J* = 2.6 Hz, 1H), 7.30 (s, 5H), 6.86 (s, 1H), 5.58 (d, *J* = 9.0 Hz, 1H), 5.06 (d, *J* = 2.3 Hz, 2H), 4.64 (d, *J* = 4.4 Hz, 2H), 4.18 (q, *J* = 8.4 Hz, 1H), 2.72 (q, *J* = 8.5 Hz, 1H), 2.58 (d, *J* = 7.3 Hz, 2H), 2.23 (qd, *J* = 9.2, 2.8 Hz, 2H); ^{13}C NMR (75 MHz, $CDCl_3$): δ 174.07, 155.52, 150.30, 148.09, 142.52, 141.51, 136.54, 128.52, 128.09, 128.09, 66.61, 42.35, 41.78, 34.39, 33.06. ESI-MS calcd for $C_{18}H_{20}ClN_4O_3^+$ 375.12 $[M+H]^+$, found 374.90.

Compound 4a-b

A reaction flask was charged with molecular sieves and heat-gun dried under high vacuum prior to use. PCl_5 (5 eq.) was added to a solution of compound **3a-b** (1 eq.) in dry ACN (0.23 M with regards to **3a-b**) at 0 °C. After overnight stirring at 50 °C, the reaction mixture was poured into ice-cold sat. $NaHCO_3$. The aqueous layer was extracted three times with EtOAc. The organic layer was dried over $MgSO_4$ and concentrated.

Benzyl (*S*)-2-(8-chloroimidazo[1,5-a]pyrazin-3-yl)pyrrolidine-1-carboxylate (4a)

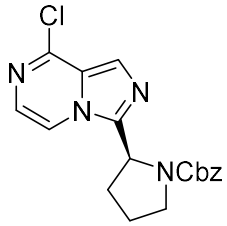

This compound was prepared from compound **3a**. The crude was purified by column chromatography (50% EtOAc in PE) to afford **4a** as a yellow oil (598 mg, 1.7 mmol, 80%). R_f= 0.3 (50% EtOAc in PE); ^{1}H NMR (300 MHz, $CDCl_3$) mixture of rotamers: δ 8.24 and 7.47 (2 d, *J* = 5.1 Hz, 1H, rotamer), 7.81 and 7.73 (2 s, 1H, rotamer), 7.40 – 7.23 and 6.95 (m and d, *J* = 5.1, 5H, rotamers), 7.18 and 6.84 (2 d, *J* = 7.4 Hz, 1H, rotamer), 5.31 and 4.75 (dd and d, 1H, rotamer), 5.14 (d, *J* = 12.2 Hz, 1H), 5.01 (d, *J* = 11.9 Hz, 1H), 3.86 – 3.55 (m, 2H), 2.61 – 2.24 and 2.18 – 1.99 (2 m, 4H, rotamers); ^{13}C NMR (75 MHz, $CDCl_3$) mixture of rotamers, resonances for minor rotamer are enclosed in parenthesis: δ 155.46 (154.09), (145.56) 145.45, (142.85) 142.70, 136.30 (135.53), 128.43 (128.33), (128.16) 128.02, 127.71, 126.79 (126.60), (125.06) 124.91, 124.44, 114.57 (113.13), (67.34) 67.11, 52.66 (52.53), (47.19) 46.54, (32.99) 31.38, 24.94 (24.15) 172.54, 154,93, 147.96, 142.37, 141.70 (141.45), 138.38, 128.31, 128.10,

127.95, 67.27, 61.15 (60.76), 47.56 (47.09), 41.85 (41.51), 31.20 (28.78), 24.59 (23.76). ESI-MS calcd for $C_{18}H_{18}ClN_4O_2^+$ 357,10 $[M+H]^+$, found 356.85.

Benzyl ((1*s*,3*s*)-3-(8-chloroimidazo[1,5-a]pyrazin-3-yl)cyclobutyl)carbamate (4b)

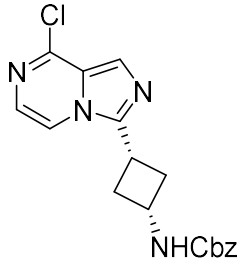

This compound was prepared from compound **3b**. The crude was purified by column chromatography (50% → 60% EtOAc in PE) to afford **4b** (106 mg, 0.30 mmol, 35%). R_f= 0.3 (50% EtOAc in PE); ^{1}H NMR (300 MHz, $CDCl_3$): δ 7.78 (s, 1H), 7.53 (d, *J* = 5.0 Hz, 1H), 7.42 – 7.09 (m, 6H), 5.57 (d, *J* = 8.6 Hz, 1H), 5.08 (s, 2H), 4.47 – 4.24 (m, 1H), 3.39 (p, *J* = 8.7 Hz, 1H), 2.90 (q, *J* = 9.4 Hz, 2H), 2.45 (qd, *J* = 9.3, 2.7 Hz, 2H); ^{13}C NMR (75 MHz, $CDCl_3$): δ 155.52, 146.11, 144.54, 136.48, 128.55, 128.17, 128.08, 127.06, 124.88, 124.58, 113.19, 66.73, 42.80, 36.48, 24.52. ESI-MS calcd for $C_{18}H_{18}ClN_4O_2^+$ 357,10 $[M+H]^+$, found 356.85.

Compound 5a-b

N-Iodosuccinimide (3 eq.) was added to a solution of compound **4a** or **4b** (1 eq.) in DMF (0.08 M) at rt. After 4h stirring at 60°C, the reaction mixture was left to reach rt. The reaction mixture was diluted in DCM and washed with a 1:1 mix of 1M $Na_2S_2O_3$ and brine. The aqueous layer was extracted with DCM. The organic phases were combined, dried over $MgSO_4$ and concentrated.

Benzyl (*S*)-2-(8-chloro-1-iodoimidazo[1,5-a]pyrazin-3-yl)pyrrolidine-1-carboxylate (5a)

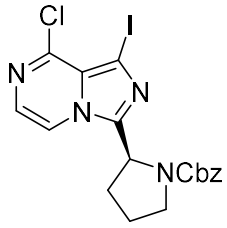

This compound was prepared from compound **4a**. The crude was purified by column chromatography (50% EtOAc in PE) to afford **5a** as a yellow oil (598 mg, 1.7 mmol, 80%). R_f= 0.3 (50% EtOAc in PE); ^{1}H NMR (300 MHz, $CDCl_3$) mixture of rotamers: δ 8.29 and 7.47 (d, *J* = 5.0 Hz, 1H, rotamer), 7.40 – 7.15 and 6.95 – 6.76 (2 m, 6H, rotamers), 5.26 – 4.89 and 4.68 (m and d, *J* = 11.8 Hz, 3H, rotamers), 3.80 – 3.44 (m, 2H), 2.60 – 2.19 and 2.14 – 1.91 (2 m, 4H, rotamers); ^{13}C NMR (75 MHz, $CDCl_3$ mixture of rotamers, resonances for minor rotamer

are enclosed in parenthesis: δ 155.61 (154.07), (145.27) 144.50, 136.28 (135.46), 128.56, (128.23) 128.15, (127.93) 127.80, 127.15 (126.97), (123.92) 123.58, 115.57 (114.02), (67.50) 67.27, (52.62) 52.55, (47.31) 46.67, (33.06) 31.54, 25.06 (24.28). ESI-MS calcd for $C_{18}H_{17}ClIN_4O_2^+$ 483.01 $[M+H]^+$, found 482.75.

Benzyl((1*s*,3*s*)-3-(8-chloro-1-iodoimidazo[1,5-a]pyrazin-3-yl)cyclobutyl)carbamate (5b)

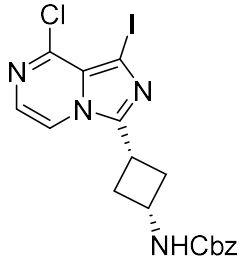

This compound was prepared from compound **4b**. The crude was purified by HPLC to afford **5b** as a white solid (100 mg, 0.20 mmol, 69%). R_f= 0.3 (50% EtOAc in PE); ^{1}H NMR (300 MHz, $CDCl_3$): δ 7.67 – 7.53 (m, 1H), 7.40 – 7.28 (m, 6H), 5.24 (s, 1H), 5.10 (s, 2H), 4.37 (d, *J* = 9.2 Hz, 1H), 3.38 (p, *J* = 9.0 Hz, 1H), 2.90 (d, *J* = 10.7 Hz, 2H), 2.54 – 2.38 (m, 2H); ^{13}C NMR (75 MHz, $CDCl_3$): δ 128.69, 128.35, 128.21, 127.52, 114.12, 66.99, 42.76, 36.51, 24.45. ESI-MS calcd for $C_{18}H_{17}ClIN_4O_2^+$ 483.01 $[M+H]^+$, found 482.75.

Compound 6a-b

In a sealed pressure tube, compound **5** was dissolved in 35% NH_4OH in H_2O (1 ml per 50 mg of compound) and dioxane (1:1 with 35% NH_4OH in H_2O). The reaction mixture was heated up to 100°C. After 3h stirring at 100°C, the reaction was concentrated and resuspended in a mix of EtOAc and 1M HCl. The organic phase was discarded and the aqueous phase was basified with sat. Na_2CO_3 to pH 8-9. The product was extracted from the aqueous phase with DCM, dried over $MgSO_4$ and concentrated.

Benzyl (*S*)-2-(8-amino-1-iodoimidazo[1,5-a]pyrazin-3-yl)pyrrolidine-1-carboxylate (6a)

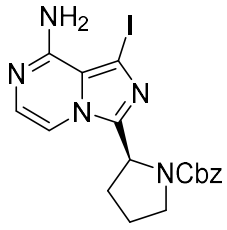

This compound was prepared from compound **5a**. The crude was purified by column chromatography (4% MeOH in DCM) to afford **6a** as a reddish solid (213 mg, 0.5 mmol, 77%). R_f= 0.3 (2% MeOH in DCM); ^{1}H NMR (300 MHz, $CDCl_3$) mixture of rotamers: δ 7.69, 7.41 – 7.15, 7.12, 7.03. 6.87 and 6.76 (d, m and 4 d, 7H, rotamers), 6.00 (br s, 2H), 5.24 – 4.94 and

4.76 (m and d, *J* = 12.0 Hz, 3H, rotamers), 3.81 – 3.54 (m, 2H), 2.48 – 2.13 and 2.07 – 1.86 (2 m, 4H, rotamers); ^{13}C NMR (75 MHz, $CDCl_3$) mixture of rotamers, resonances for minor rotamer are enclosed in parenthesis: δ 155.3 (154.34), 151.14, 143.93, 136.58 (135.96), 128.57 (128.47), 128.37 (128.30), 128.12, 127.87, (119.15) 118.86, 108.34 (107.31),74.50 (67.28) 67.15, (52.97) 52.80, (47.28) 46.67, (32.94) 31.64, 24.94 (24.21). ESI-MS calcd for $C_{18}H_{19}ClIN_5O_2^+$ 464.06 $[M+H]^+$, found 463.80.

Benzyl((1*s*,3*s*)-3-(8-amino-1-iodoimidazo[1,5-a]pyrazin-3-yl)cyclobutyl)carbamate (6b)

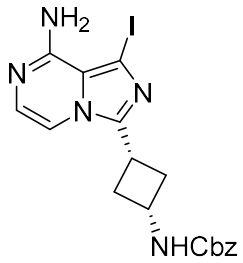

This compound was prepared from compound **5b**. The crude was purified by purified by column chromatography (4% MeOH in DCM) to afford **6b** as a white solid (36.2 mg, 0.08 mmol, 39%). R_f= 0.25 (4% MeOH in DCM); ^{1}H NMR (300 MHz, $CDCl_3$): δ 7.35 (s, 5H), 7.13 (d, *J* = 5.1 Hz, 1H), 7.03 (d, *J* = 5.4 Hz, 1H), 5.88 (br s, 2H), 5.38 (d, *J* = 9.1 Hz, 1H), 5.09 (s, 2H), 4.36 (q, *J* = 8.6 Hz, 1H), 3.31 (p, *J* = 8.5 Hz, 1H), 2.87 (d, *J* = 10.2 Hz, 2H), 2.39 (qd, *J* = 9.2, 2.8 Hz, 2H); ^{13}C NMR (75 MHz, $CDCl_3$): δ 151.25, 128.66, 128.58, 128.28, 128.24, 107.19, 66.85, 42.77, 36.56, 24.41. ESI-MS calcd for $C_{18}H_{19}ClIN_5O_2^+$ 564.05 $[M+H]^+$, found 563.80.

Compound 7a-b

In a flask containing compound **6a-b** (34 mg, 0.14 mmol, 1 eq.) and compound **11a-b** (65 mg, 0.14 mmol, 1 eq.) in DME (1 mL per 0.06 mmol of compound **6**, degassed by stream of N_2), K_2CO_3 (42 mg, 0.31 mmol, 2.2 eq.) and $Pd(PPh_3)_4$ (9 mg, 5 mol%) were added, followed by addition of water (320 µL per 0.06 mmol of compound **6**, degassed by stream of N_2). The reaction mixture was stirred overnight at 80 °C. The solvents were then removed and the crude product was purified by column chromatography.

(*S*)-benzyl 2-(8-amino-1-(4-(pyridin-2-ylcarbamoyl)phenyl)imidazo[1,5-*a*]pyrazin-3-yl)pyrrolidine-1-carboxylate (7a)

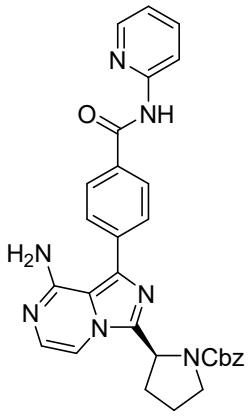

This compound was prepared from compounds **6a** and **12a** and the crude was purified by column chromatography (3 % MeOH in DCM) to give **7a** as a yellow solid (39 mg, 0.07 mmol, 52% yield). ^{1}H NMR (500 MHz, $CDCl_3$) mixture of rotamers: δ 8.78 (d, *J* = 8.7 Hz, 1H), 8.29 (d, *J* = 5.5 Hz, 1H), 8.24 (d, *J* = 8.0 Hz, 2H), 8.13 (t, *J* = 8.2 Hz, 1H), 7.89, 7.80, 7.71 and 7.69 (4 d, 3H, rotamers), 7.40 – 7.27 (m, 4H), 7.24 – 7.18 (m, 1H), 7.09, 6.96, 6.85 and 6.45 (4 d, 2H, rotamers), 6.13 (br s, 2H) 5.28 – 5.00 and 4.71 (m and d, 3H, rotamers), 3.84 – 3.61 (m, 2H), 2.61 – 2.32 and 2.15 – 2.02 (2 m, 4H, rotamers). ^{13}C NMR (126 MHz, $CDCl_3$) mixture of rotamers, resonances for minor rotamer are enclosed in parenthesis: δ 165.53, 164.46, 164.17, 155.51, 150.57, 150.08, 146.48, 143.18, 143.00, 141.91, 136.66, 134.05, 129.56, 129.34, 128.48, 128.16, 127.76, 120.04, 117.14, 115.17, 108.84 (107.29), (67.55) 67.33, 52.38, (47.29) 46.65, (33.07) 31.50, 25.00 (24.20). ESI-MS calcd for $C_{30}H_{28}N_7O_3^+$ 533.59 $[M+H]^+$, found 534.00.

Benzyl ((1*s*,3*s*)-3-(8-amino-1-(2-phenylquinolin-7-yl)imidazo[1,5-*a*]pyrazin-3-yl)cyclobutyl)carbamate (7b)

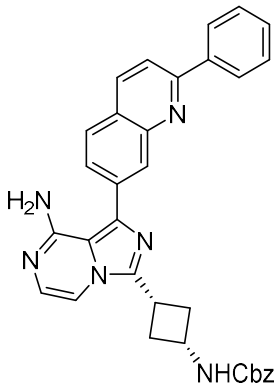

This compound was prepared from compounds **6b** and **12b** and the crude was purified by column chromatography (2-4 % MeOH in DCM) to give **7b** as a yellow solid (21 mg, 0.39 µmol, 50% yield). ^{1}H NMR (500 MHz, $CDCl_3$) δ 8.61 (s, 1H), 8.51 (d, *J* = 8.7 Hz, 1H), 8.15 – 8.09 (m, 3H), 8.07 (d, *J* = 8.3 Hz, 1H), 8.02 (d, *J* = 8.7 Hz, 1H), 7.92 (d, *J* = 8.3 Hz, 1H), 7.59 – 7.48 (m, 3H), 7.38 – 7.24 (m, 4H), 7.16 (d, *J* = 5.7 Hz, 1H), 6.83 (d, *J* = 5.9 Hz, 1H), 5.42 (d, *J* = 8.7 Hz,

1H), 5.08 (s, 2H), 4.40 (q, *J* = 8.4 Hz, 1H), 3.40 (p, *J* = 8.7 Hz, 1H), 3.01 – 2.84 (m, 2H), 2.59 – 2.46 (m, 2H). 13C NMR (126 MHz, $CDCl_3$) δ 162.42, 162.12, 157.74, 155.40, 150.45, 148.30, 144.39, 142.89, 140.22, 136.30, 135.42, 131.28, 129.47, 129.22, 128.48, 128.25, 128.10, 127.99, 127.43, 126.74, 120.95, 116.98, 115.62, 114.67, 112.07, 107.19, 66.70, 42.66, 36.35, 24.19.ESI-MS calcd for $C_{33}H_{29}N_6O_2^+$ 541.61 $[M+H]^+$, found 541.00.

Compound 8a-b

In a flask containing compound **7a/b** (1 eq.) in DCM (1 mL per 0.054 mmol of compound **7**), Fmoc-Cl (20 eq.) and pyridine (20 eq.) were added and the reaction mixture was stirred overnight at RT. The solvent was then removed and the crude product was purified by column chromatography (for **8a**) or used crude **(8b**).

(*S*)-benzyl 2-(8-((((9H-fluoren-9-yl)methoxy)carbonyl)amino)-1-(4-(pyridin-2-ylcarbamoyl)phenyl)imidazo[1,5-a]pyrazin-3-yl)pyrrolidine-1-carboxylate (8a)

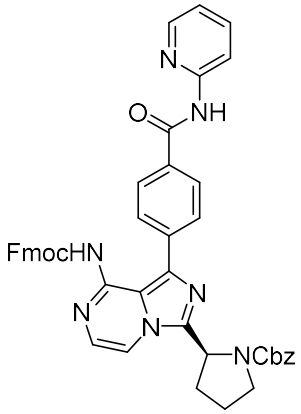

This compound was prepared from compound **7a** and the crude was purified by column chromatography (0-20 % MeOH in DCM) to give **8a** as a yellow solid (5.61 mg, 0.007 mmol, 10% yield). ^{1}H NMR (600 MHz, $CDCl_3$) mixture of rotamers: δ 8.83 (t, *J* = 9.7 Hz, 1H), 8.28 (m, 1H), 8.16 (s, 3H), 8.09 and 8.00 (2 m, 1H, rotamer), 7.79 – 7.66 and 7.65 – 7.55 (2 m, 4H, rotamers), 7.42 – 7.13 (m, 12H, contains $CDCl_3$ peak), 6.96 and 6.55 (2 s, 1H, rotamer), 5.33 – 5.26, 5.17 – 5.00 and 4.80 – 4.76 (3 m, *J* = 11.8 Hz, 3H, rotamers), 4.33 – 4.26 and 4.26 – 4.15 (2 m, 2H, rotamers), 3.82 – 3.60 (m, 2H, rotamers), 2.59 – 2.50, 2.48 – 2.31 and 2.12 – 2.05 (3 m, 4 H, rotamers). ^{13}C NMR (151 MHz, $CDCl_3$) mixture of rotamers, resonances for minor rotamer are enclosed in parenthesis: δ 166.40, 163.27, 155.62, 150.12, 144.00, 143.76, 143.68, 141.20, 140.42, 138.63, 136.31, 131.88, 130.52, 128.50, 128.11, 127.79, 127.65, 127.09, 125.33, 124.68, 120.07, 119.83, 119.59, 117.74, 68.10, (67.54) 67.26, (52.74), 52.43, (47.32) 46.70, 46.62, (33.05) 31.54, 25.06 (24.24). ESI-MS calcd for $C_{45}H_{38}N_7O_5^+$ 756.29 $[M+H]^+$, found 756.20.

Benzyl ((1*s*,3*s*)-3-(8-((((9H-fluoren-9-yl)methoxy)carbonyl)amino-1-(2-phenylquinolin-7-yl)imidazo[1,5-*a*]pyrazin-3-yl)cyclobutyl)carbamate (8b)

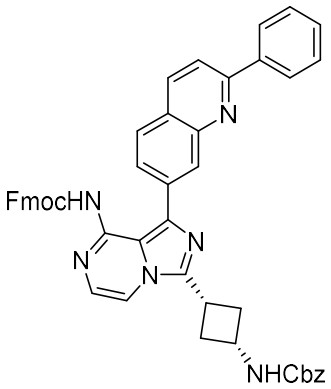

This compound was prepared from compound **7b**, and was used in the next step without further purification, because the Fmoc-protecting group turned out to be instable during purification. ESI-MS calcd for $C_{48}H_{39}N_6O_4^+$ 763.31 $[M+H]^+$, found 763.30.

Compound 9a-b

To an ice-cold a flask containing compound **8a/b** (1 eq.), 33% HBr in AcOH (100 µL per 4 mg of compound **8a/b**) was added and the reaction was stirred for 1 hour at rt. The reaction mixture was co-evaporated with toluene. The crude product was dissolved in DMF (0.25 M final concentration) and basified by addition of DIPEA (flask 1). In a separate flask (flask 2), compound **13** (1.1 eq. with regards to compound **9**) was dissolved in DMF (0.3 M final concentration) followed by addition of HATU (1.1 eq.) and DIPEA (3 eq.). After 10 minutes, the deprotected crude amine from flask 1 was transferred to flask 2 and the reaction stirred overnight at RT. At this point, DBU (1 % in DMF, 3 eq.) were added to the reaction mixture and the reaction was stirred for another hour at RT. The solvent was then evaporated and the crude was purified by preparative HPLC.

(S)-4-(8-amino-3-(1-(3-(3-(but-3-yn-1-yl)-3H-diazirin-3-yl)propanoyl)pyrrolidin-2-yl)imidazo[1,5-a]pyrazin-1-yl)-N-(pyridin-2-yl)benzamide (9a)

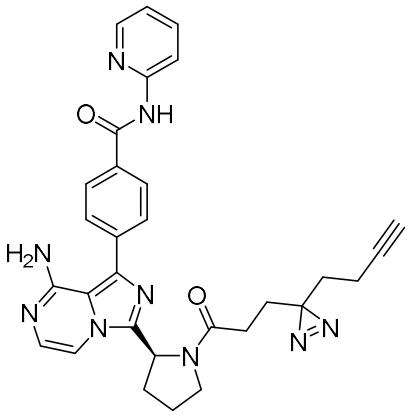

This compound was prepared from compounds **8a** and **12**. The crude product was purified by preparative HPLC to give final product **9a** as a yellow solid (1.0 mg, 1.8 µmol, 25 % yield over 3 steps). Because of the obtained quantities and the presence of rotamers around the amide bond, a full characterization was not performed. Calculated LC-purity: 99%. HRMS calcd for $C_{30}H_{30}N_9O_2^+$ 548.2444 $[M+H]^+$, found 548.2513.

_N_-((1s,3s)-3-(8-amino-1-(2-phenylquinolin-7-yl)imidazo[1,5-a]pyrazin-3-yl)cyclobutyl)-3-(3-(but-3-yn-1-yl)-3H-diazirin-3-yl)propenamide (9b)

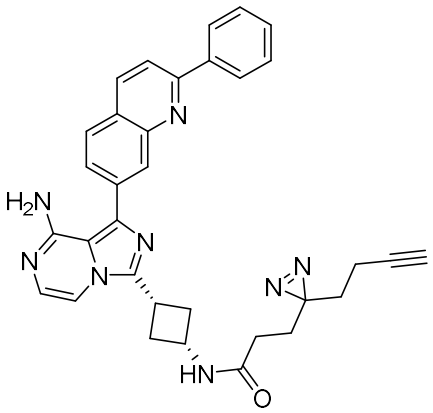

This compound was prepared from compounds **8b** and **12**. The crude product was purified by preparative HPLC to give final product **9b** as a yellow solid (1.0 mg, 1.8 µmol, 18 % yield over 4 steps). Because of the obtained quantities, a full characterization was not performed. Calculated LC-purity: 93%. HRMS calcd for $C_{33}H_{31}N_8O^+$ 555.2576 $[M+H]^+$, found 555.2614. ^{1}H NMR (600 MHz, $CDCl_3$): δ 8.43 (d, *J* = 1.6 Hz, 1H), 8.33 (d, *J* = 8.6 Hz, 1H), 8.23-8.20 (m, 2H), 8.05 (d, *J* = 8.5 Hz, 1H), 8.02 (d, *J* = 8.6 Hz, 1H), 7.79 (dd, *J* = 1.7 Hz, *J* = 8.3 Hz, 1H), 7.58-7.54 (m, 2H), 7.53-7.50 (m, 1H), 7.20 (d, *J* = 5.9 Hz, 1H), 6.86 (d, *J* = 5.9 Hz, 1H), 6.02 (d, *J* = 8.2 Hz, 1H), 4.64 (sext, *J* = 8.2 Hz, 1H), 3.54-3.47 (m, 1H), 3.03-2.97 (m, 2H), 2.57-2.51 (m, 2H), 2.03-1.97 (m, 3H), 1.94-1.90 (m, 2H), 1.86-1.82 (m, 2H), 1.63 (t, *J* = 7.3 Hz, 2H).

Supplemental references

1. Uhlen, M. *et al.* Towards a knowledge-based Human Protein Atlas. *Nature Biotechnology* vol. 28 1248–1250 (2010).
2. Schneider, C. A., Rasband, W. S. & Eliceiri, K. W. NIH Image to ImageJ: 25 years of image analysis. *Nat Methods* **9**, 671–675 (2012).
3. Perez-Riverol, Y. *et al.* The PRIDE database and related tools and resources in 2019: Improving support for quantification data. *Nucleic Acids Res.* **47**, D442–D450 (2019).
4. Project Jupyter. *https://jupyter.org/*.
5. Bisong, E. *Building Machine Learning and Deep Learning Models on Google Cloud Platform*. *Building Machine Learning and Deep Learning Models on Google Cloud Platform* (Apress, 2019). doi:10.1007/978-1-4842-4470-8.
6. Arantes, P. R., Polêto, M. D., Pedebos, C. & Ligabue-Braun, R. Making it Rain: Cloud-Based Molecular Simulations for Everyone. *J. Chem. Inf. Model.* **61**, 4852–4856 (2021).
7. Morris, G. M. *et al.* AutoDock4 and AutoDockTools4: Automated docking with selective receptor flexibility. *J. Comput. Chem.* **30**, 2785–2791 (2009).
8. Trott, O. & Olson, A. J. AutoDock Vina: improving the speed and accuracy of docking with a new scoring function, efficient optimization, and multithreading. *J. Comput. Chem.* **31**, 455–461 (2010).